# ABELL 2631 MeerKAT Deep source catalog with source counts

Robert Kincaid

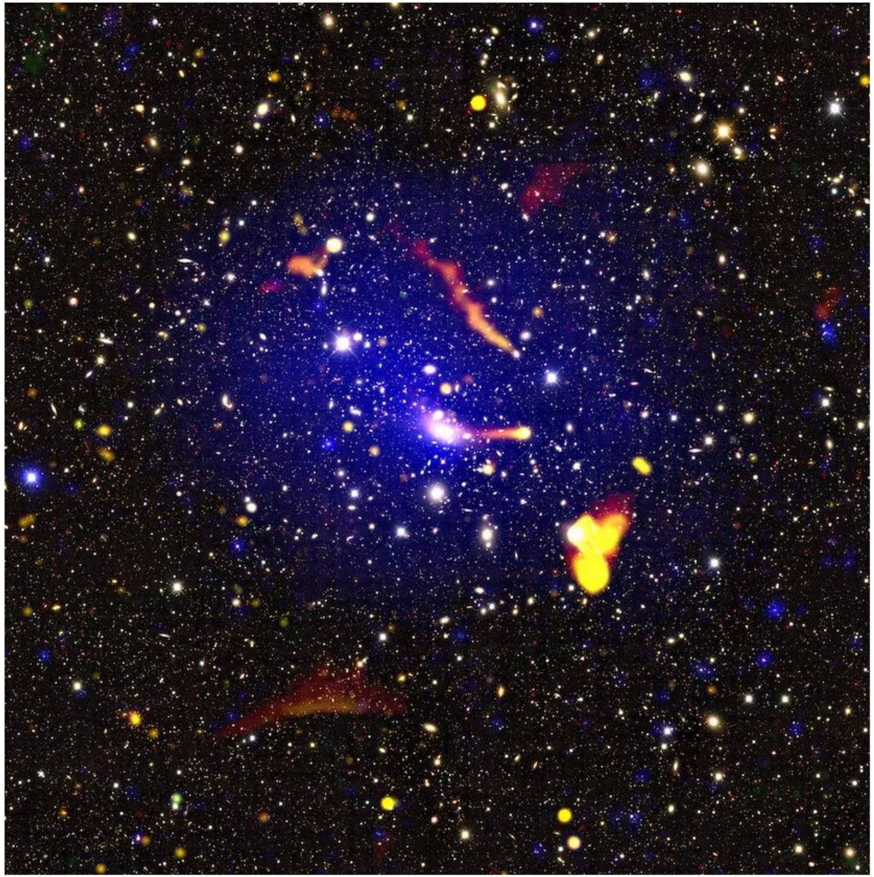

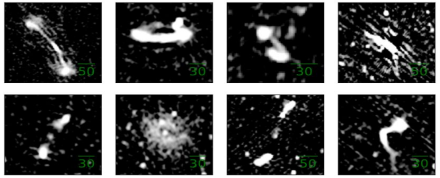

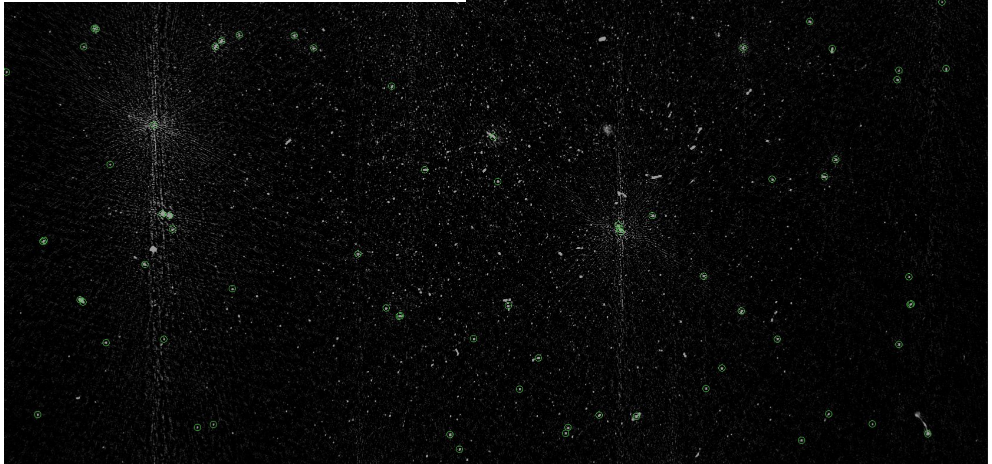

# Radio source counts

- Curve produced by counts of radio sources per unit area as a function of flux density were one of the earliest cosmological probes.
- These curves can tell us the relative populations of galaxy types and cosmological evolution from the luminosity function.
- Inflection point ~ 1mJy signalling the emergence of a new population of galaxies.
- There is no census on the relative galaxy populations on this faint sub mJy regime where counts show a turn up.
- Turn up indicates an increasing dominance of star forming galaxies over AGN at lower lumosities.

| Euclidean and static Universe | non-Euclidean and evolving Universe |
| --- | --- |
| $n(S) \propto S^{-3/2}$ | $\log(dN/dS) \propto \sum_{i=0}^{N} a_i [\log(S)]^i$ |
| Constant Comoving source density -> non-evolving sources | Changing comoving source density |

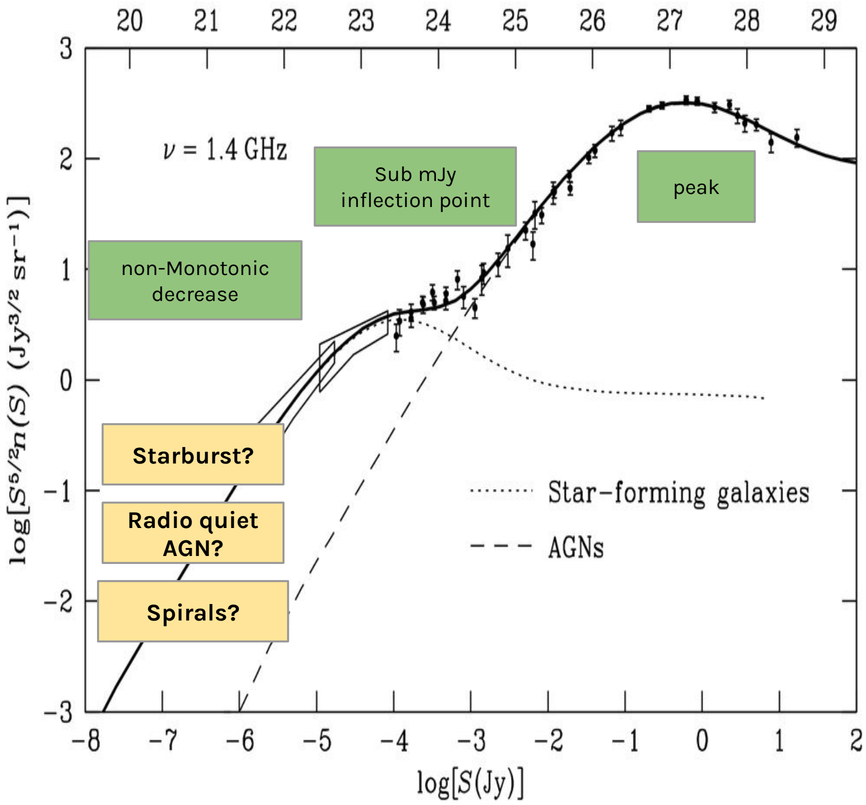

# MeerKAT observation of A2631

- 8 hour observations (4096 channels, 16s int time) of Abell 2631, the largest galaxy cluster residing in the core of the saraswati supercluster (z~0.27).
- Resolution of about 8” with sensitivity down to 0.01 mJy.
- Sample of ~ 3000 radio sources with flux density 15uJy to 10mJy on pb cut image. (Image cut where pb response < 50-60%).
- A2631 scenario unclear. Contains bright AGN and disturbed X-ray morphology -> merging galaxy cluster?
- One of the most significant density enhancements found at medium-to-high redshifts (z ~ 0.27, universe ~ 10 billion years old).
- Is similar to the well-known Shapley and Virgo superclusters.

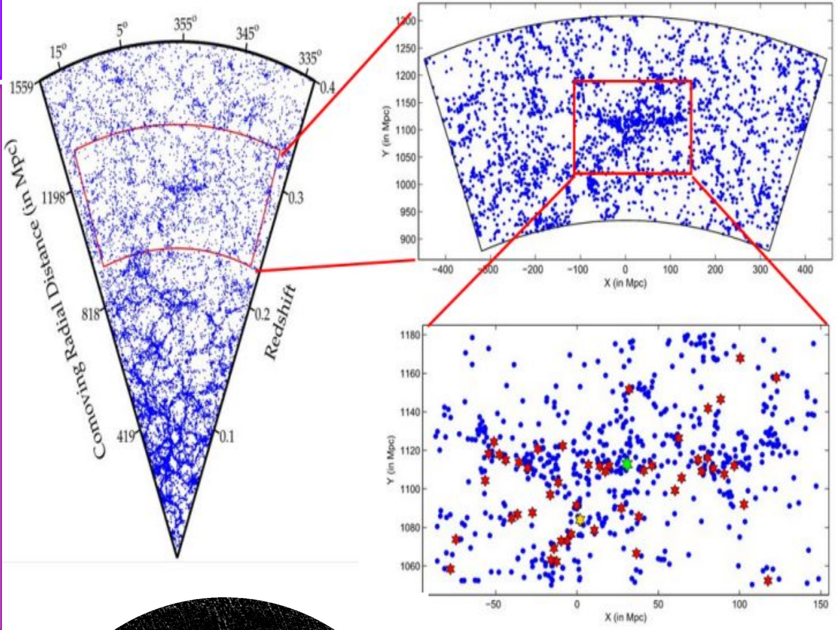


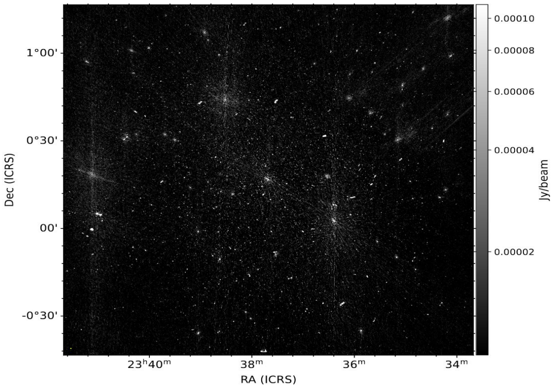


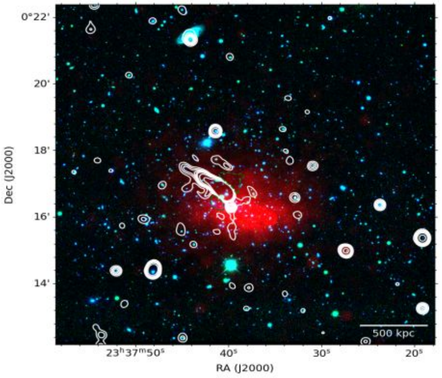


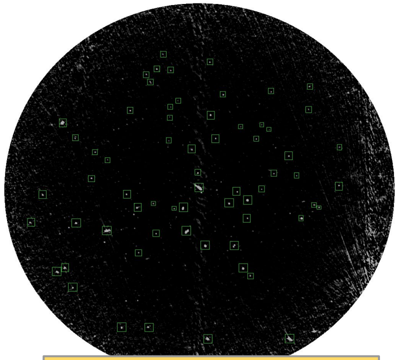

Primary beam cut ~ 1deg^2

Table 3.1: MeerKAT observations of the *Saraswati* supercluster.

| | |
|---|---|
| Observation date: | 2019-06-15 |
| Observation time: | 00:41:27.8 |
| Number of pointings: | 2 |
| Phase centre of A2631 (J2000): | RA: $23^h37^m40.60^s$, DEC: $+00°16'36.0''$ |
| Phase centre of ZwCl 2341 (J2000): | RA: $23^h43^m39.70^s$, DEC: $+00°19'51.0''$ |
| Number of antennas: | 60 |
| Total observation time: | 14 hours |
| Central frequency: | 1283 MHz |
| Total bandwidth: | 900 MHz |
| Channel width: | 208 kHz |
| Total number of channels: | 4016 |
| Dump time: | 16s |
| Cross products: | XX, XY, YX, YY |
| Band pass and flux calibrator: | J1939-6342 |
| J1939-6342 coordinates (J2000): | RA: $19^h39^m25.02^s$, DEC: $-63°42'45.62''$ |
| J1939-6342 flux density at 1.4 GHz: | ~ 14.90 Jy |
| Gain calibrator: | J2357-1125 |
| J2357-1125 coordinates (J2000): | RA: $23^h57^m31.25^s$, DEC: $-11°25'38.90''$ |
| J2357-1125 flux density at 1.4 GHz: | ~ 1.80 Jy |

# Correcting for the biases introduced from observations

- Address the biases introduced from the observation and cataloging process.
- Incompleteness results from varying rms levels due to the primary beam and uneven noise distribution.
- For correcting incompleteness we need to perform simulations with real source size and flux distribution injected on a residual noise map.
- In addition to incompleteness we have various other errors that must be accounted for.
- Resolution bias: Preferential non-detection of large sources.
- Resolved extended sources can more easily fall below peak threshold while integrated flux does not.
- Smearing: Finite bandwidth causes sources further from phase centre to be “smeared”.
- Cosmic variance cosmological in origin (non-poisson).

## Correction effects

- Noise bias
- Resolution bias
- False detection rate
- smearing
- Cosmic variance

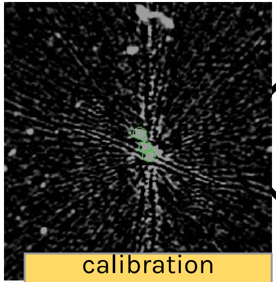

calibration artifacts

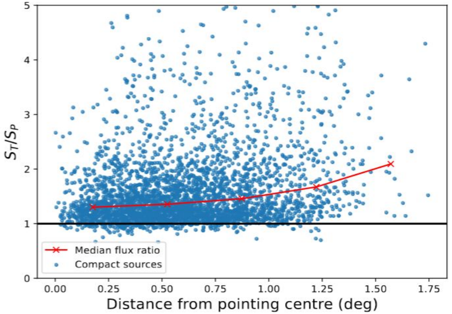


Smearing

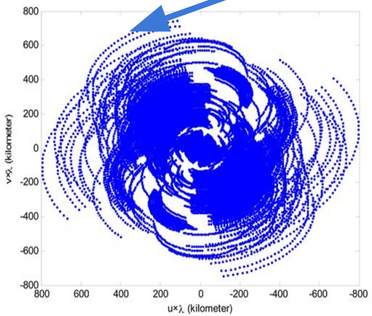


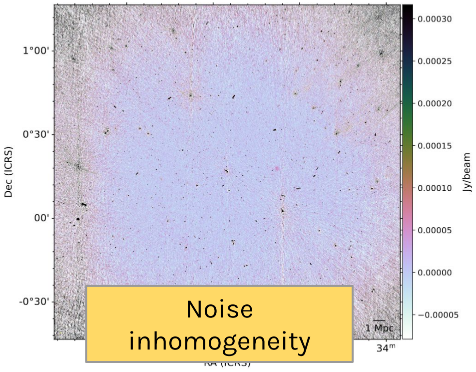


Noise inhomogeneity

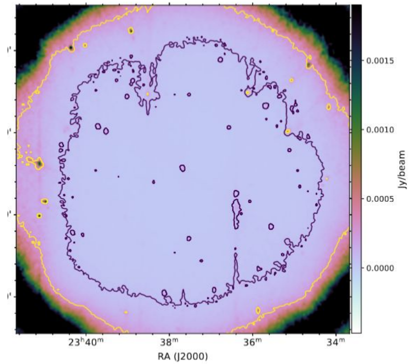

# The effect of Cosmic variance on small survey areas

- Combined source count data of previous single pointing data show significant scatter at faint end compared to larger survey areas.
- At smaller areas the underlying cosmological structure can have a noticeable effect on the radio source properties.
- Deeper depths are required for single pointing to achieve the same scatter of that for larger area.



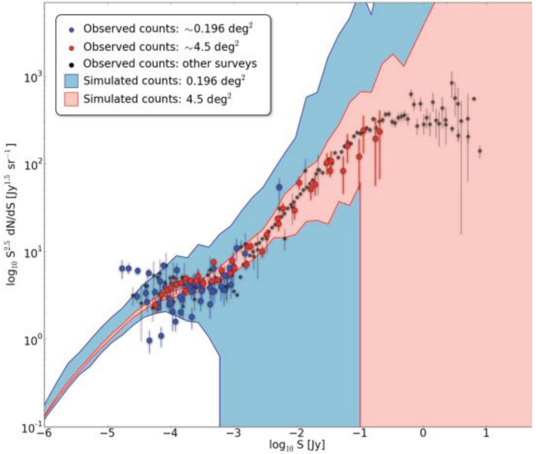


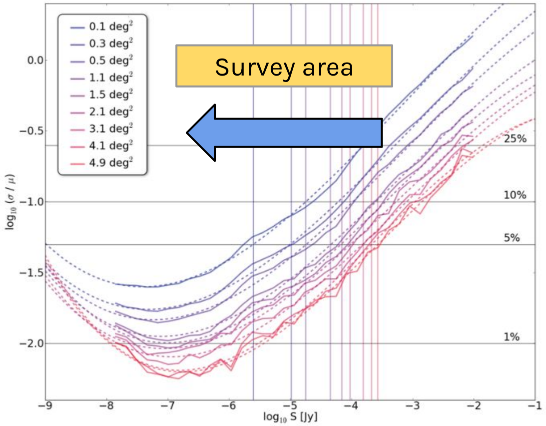

# Procedure for deriving the completeness function

- One of the resultant products of the CLEAN algorithm is the residual image. After deep cleaning should contain no sources and just noise.
- Simulated sources with real flux and source size are injected into the  residual image. Source finder used on this simulated image with the same parameters as real image.
- PyBDSF source finder software] searches for  islands of emissions in which gaussians are subsequently fitted based on peak flux and image noise distribution.
- By counting the sources for each bin and computing the ratio: injected_sources/Recovered sources we obtain correction factors per flux density bin.

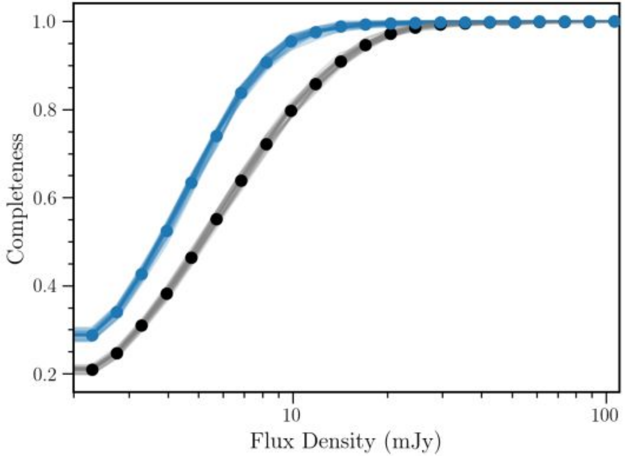


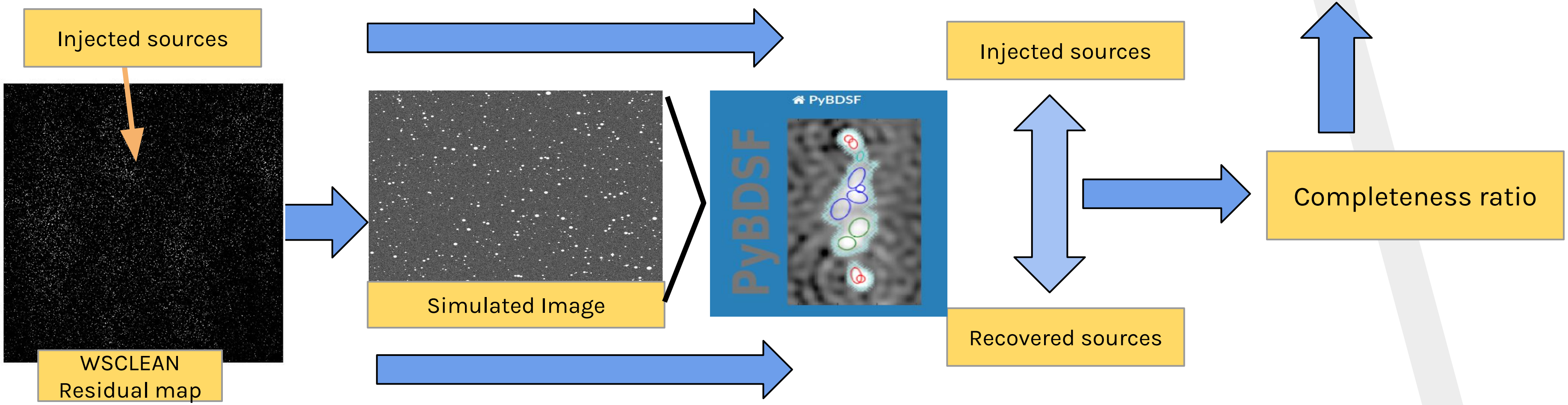

# Simulation details: Radio flux and source size selection

## Flux selection

- Inverse Transfer sampling used to choose from a uniform sample of points from a continuous distribution.
- Calculate the Inverse of the cumulative distribution function and then evaluate this function from a normalised uniform sample.
- Total sources injected into simulated image determined by integration of source count function.

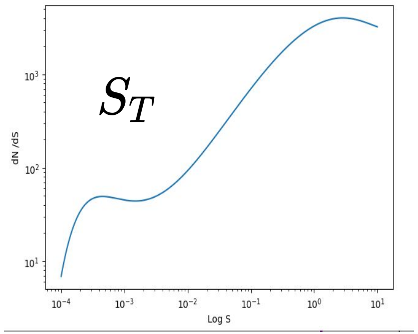


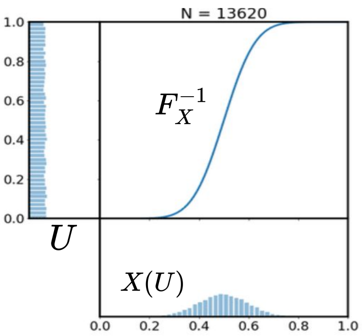


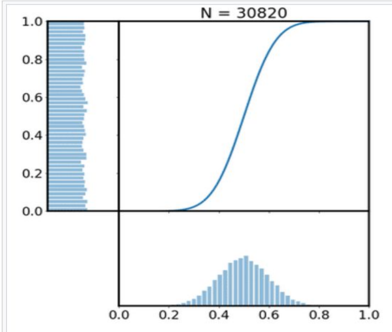


$$\log\left[(dN/dS)\ S^{2.5}\right] = \sum_{i=0}^{4} a_i\ \left[\log(S)\right]^i ,$$

$$h(>\Theta) = \exp[-\ln 2\,(\Theta/\Theta_{\rm med})^q]$$

$$N = \int_{2\sigma}^{max} 10^{\sum_{i=0}^{N} a_i[\log(S)]^i}\, dS \quad X(u) = F_X^{-1}(u) \quad U \in [0, 1, N] \quad X(U) = F_X^{-1}(U)$$

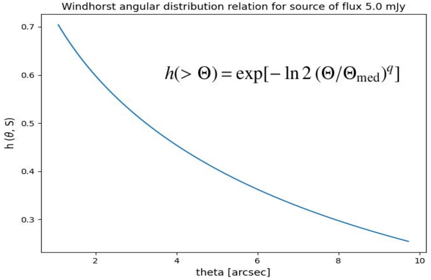


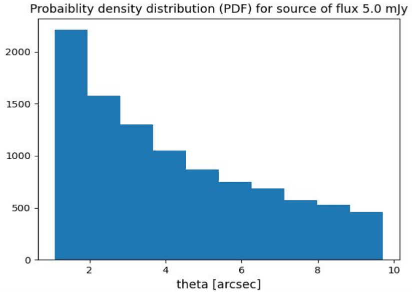


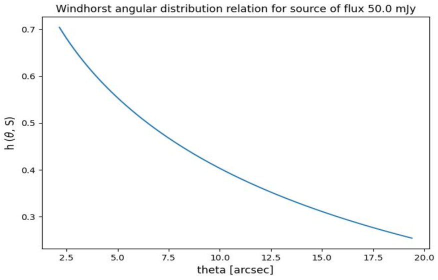


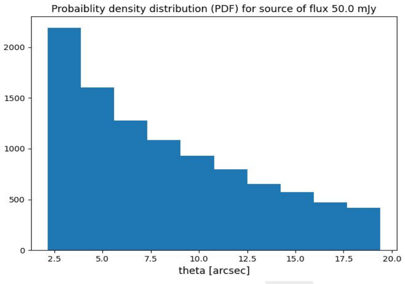


## Source size selection

- Windhorst relation most widely used: Empirical integral distribution that shows a decline in angular sizes for fainter sources.
- A source of a given flux will have a range of angular sizes to be chosen from.
- Larger fluxes will have larger angular sizes and vica versa.

# Simulation details: Injection of gaussian sources

- We injected circular gaussian sources for simplicity and for each assign a peak flux.
- The peak flux must then be spread across the source size for the integrated flux
- Source size depends on beam size and true intrinsic size
- True size is the source size found from angular source size model such as Windhorst

$$f(x,y) = A\exp\left(-\left(\frac{(x-x_0)^2}{2\sigma_X^2} + \frac{(y-y_0)^2}{2\sigma_Y^2}\right)\right).$$

$$A = S_P = S_T \times \left(\frac{\text{area\_s}}{\text{area\_b}}\right)$$

$$\text{area\_s} = \sigma_X = \sigma_Y = MAJ * MIN \quad \text{area\_b} = BMAJ * BMIN$$

$$MAJ = \sqrt{BMAJ^2 + maj^2}$$

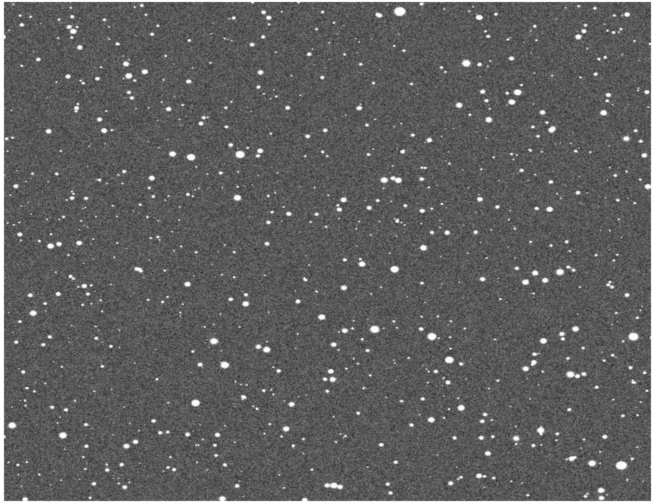

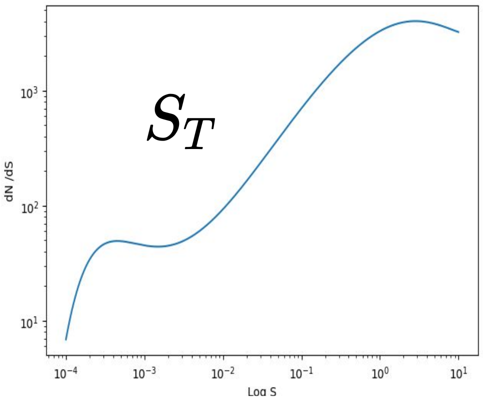


$$\log\left[(dN/dS)\, S^{2.5}\right] = \sum_{i=0}^{4} a_i \left[\log(S)\right]^i,$$

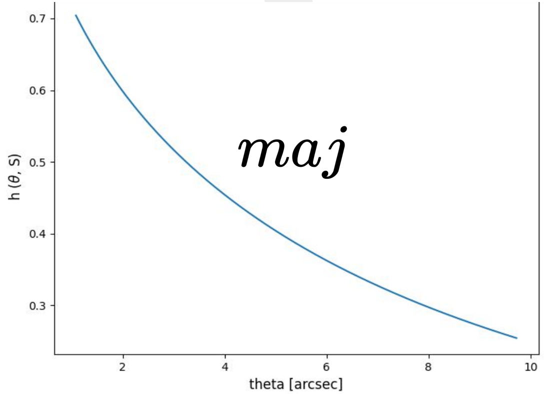


$$h(>\Theta) = \exp[-\ln 2\, (\Theta/\Theta_{\rm med})^q]$$

# Resolved and unresolved sources

- In an ideal image (absence of noise) total flux of a point source is equal to peak flux. For an extended source Total flux > peak flux.
- In real images total flux and peak are changed by the noise, smearing, primary beam, noise peaks, etc
- Sources with S_T <  S_P are affected with errors. Can assume by extension that errors affects sources with  S_P > S_T as well.
- Can fit a lower envelope for 90%, 95% or 97% of sources S_T < S_P.

$$S_{\text{total}}/S_{\text{peak}} = \text{A} \cdot (1 + \text{B}/(S/N)).$$

$$S_{\text{total}}/S_{\text{peak}} = \theta_{\text{maj}}\theta_{\text{min}}/b_{\text{min}}b_{\text{maj}}$$

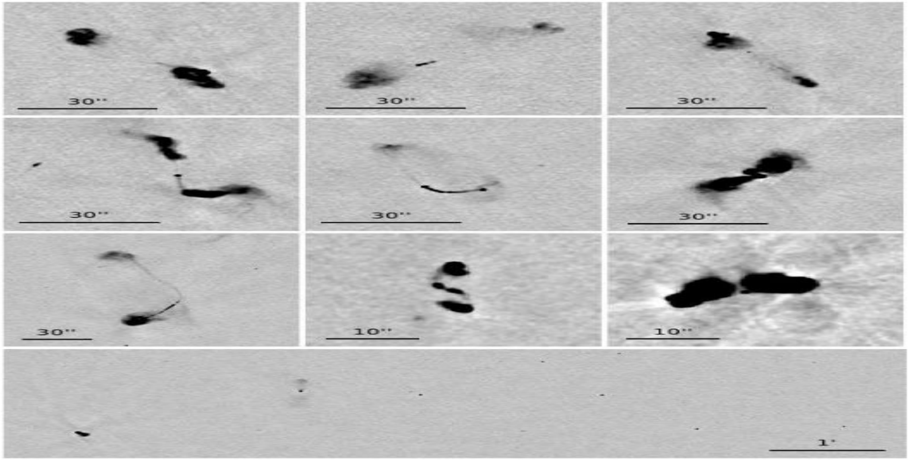


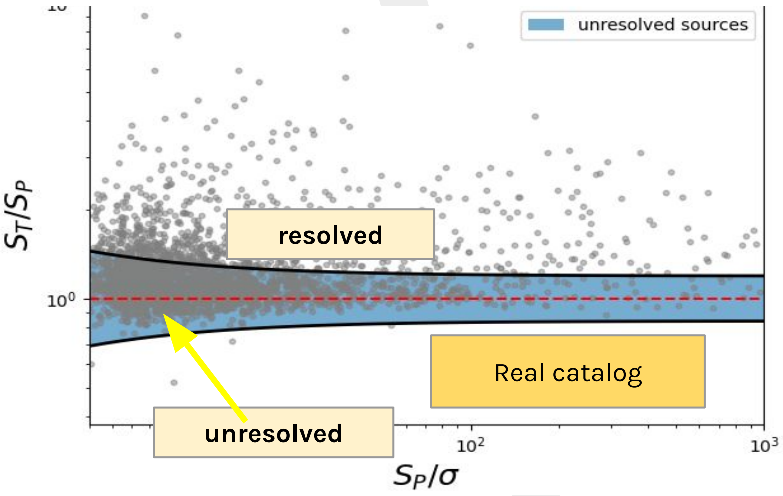


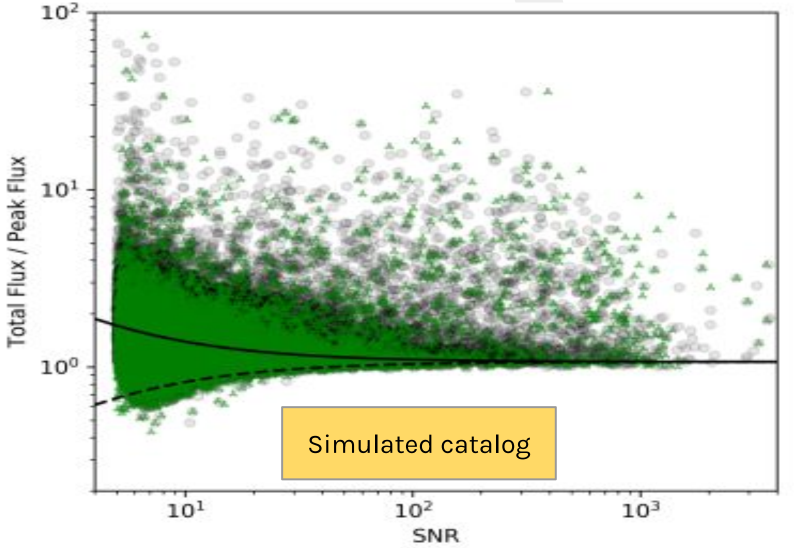

# Completeness and source counts

- MeerKAT radio source counts compared with Deep observations from GMRT and VLA scaled to 1.4GHz (alpha =-0.7)
- GMRT comparable to MeerKAT in terms of sensitivity (~0.03mJy) and resolution (~ 10”).
- GMRT data able to populate the higher luminosities but not deep enough to explore the transition region ~ 1 mJy.
- MeerKAT data provide a wealth of uJy - mJy sources allowing us to probe transition region.
- Application of 1/completeness shifts sources in the lower bins up while minimal effect on bright sources.
- Optical crossmatch required to understand the full nature of sources below the transition zone.
- Future SKA and SKA-precursors will be vital to uncover the true nature of radio galaxies in this regime.